



Stereoselective metabolism of chloramphenicol by bacteria isolated from wastewater, and the importance of stereochemistry in environmental risk assessments for antibiotics

Felicity C T Elder^a, Ben Pascoe^b, Stephen Wells^{a,c}, Samuel K Sheppard^b, Jason Snape^d, William H Gaze^e, Edward J Feil^b, Barbara Kasprzyk-Hordern^{a,*}

^a Department of Chemistry, University of Bath, BA27AY, Bath, UK

^b The Milner Centre for Evolution, Department of Biology and Biochemistry, University of Bath, BA27AY, Bath, UK

^c Department of Chemical Engineering, University of Bath, BA27AY, Bath, UK

^d AstraZeneca Global Sustainability, Mereside, Macclesfield, SK104TG, UK

^e European Centre for Environment and Human Health, University of Exeter Medical School, ESI, University of Exeter, Penryn Campus, Penryn, TR10 9FE, UK

ARTICLE INFO

Keywords:

Antibiotics
Stereochemistry
Chirality
Transformation
AMR
Environment
Wastewater

ABSTRACT

Wastewater treatment plants have been highlighted as a potential hotspot for the development and spread of antibiotic resistance. Although antibiotic resistant bacteria in wastewater present a public health threat, it is also possible that these bacteria play an important role in the bioremediation through the metabolism of antibiotics before they reach the wider environment. Here we address this possibility with a particular emphasis on stereochemistry using a combination of microbiology and analytical chemistry tools including the use of supercritical-fluid chromatography coupled with mass spectrometry for chiral analysis and high-resolution mass spectrometry to investigate metabolites. Due to the complexities around chiral analysis the antibiotic chloramphenicol was used as a proof of concept to demonstrate stereoselective metabolism due to its relatively simple chemical structure and availability over the counter in the U.K. The results presented here demonstrate the chloramphenicol can be stereoselectively transformed by the chloramphenicol acetyltransferase enzyme with the orientation around the first stereocentre being key for this process, meaning that accumulation of two isomers may occur within the environment with potential impacts on ecotoxicity and emergence of bacterial antibiotic resistance within the environment.

1. Introduction

Antibiotics (ABs) have revolutionised healthcare, animal husbandry, agriculture and aquaculture since their discovery over a hundred years ago. Over the 30 years there has been a dramatic increase in the reporting of antibiotic resistance bacteria (ABR) leading the World Health Organisation to recognise ABR as a global health threat.

The focus on the therapeutic role of ABs and the clinical implications of antibiotic resistance (ABR) has led us to often overlook the fact that antibiotic biosynthetic genes and antibiotic resistance genes (ARGs) have co-evolved over millennia, leading to a reservoir of ARGs within the environment (González-Zorn and Escudero, 2012). This linked with the increasing presence of antibiotics within the environment due to poor stewardship has led to the increasing need to understand the role

different environmental compartments play in the development and spread of antibiotic resistance (Manaia *et al.*, 2018; Qiao *et al.*, 2018). It is also important to understand the fate of antibiotics within the environment including how ABs are degraded or metabolised by micro-organisms. Here we focus on the microbial transformation of the antibiotic chloramphenicol, with specific focus on the role of stereochemistry and chirality.

Stereochemistry is the study of the 3-dimensional shape of molecules through the study of the relative spatial arrangement of atoms within the molecule, whilst chirality refers to the cases whereby a molecule is not superimposable on its mirror image (Helmchen, 2016). Pure enantiomers of chiral compounds exhibit the same physiochemical properties but due to their difference in 3-dimensional shape their behaviour within biochemical processes can be strikingly different. This is because

* Corresponding author.

E-mail address: b.kasprzyk-hordern@bath.ac.uk (B. Kasprzyk-Hordern).

<https://doi.org/10.1016/j.watres.2022.118415>

Received 8 October 2021; Received in revised form 1 March 2022; Accepted 4 April 2022

Available online 6 April 2022

0043-1354/© 2022 The Author(s). Published by Elsevier Ltd. This is an open access article under the CC BY license (<http://creativecommons.org/licenses/by/4.0/>).

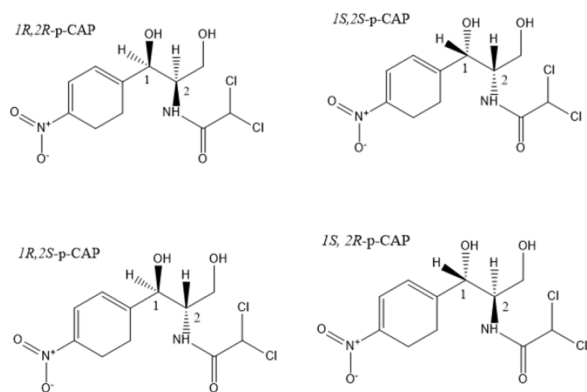


Fig. 1. Chloramphenicol isomers

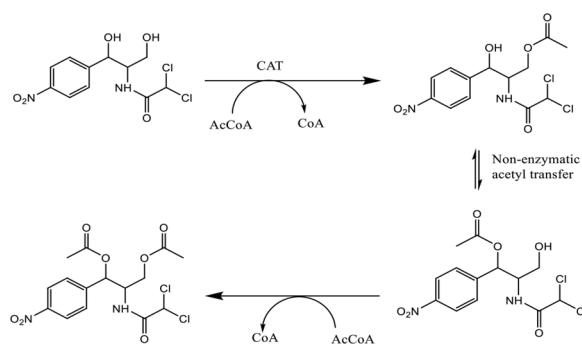


Fig. 2. CAT acetylation of chloramphenicol

the biological world is 3-dimensional and therefore fundamentally chiral. The fact that the 'living world' is fundamentally chiral has been exploited in the production of enantiomerically pure drugs (Honma et al., 1979; Koeller and Wong, 2001; Fessner et al., 2015) and environmental bacterial metabolism of pharmaceuticals including fluoxetine, ephedrine and amphetamines has been shown to be stereoselective (Bagnall et al., 2013; Ribeiro et al., 2013; Evans, Bagnall and Kasprzyk-Hordern, 2016; Andrés-Costa et al., 2017; Rice et al., 2018). The enantiomeric composition of ofloxacin in the aqueous environment was investigated by Castrignano et al (Castrignano et al., 2018), where it was shown that there was an enrichment of *S*-(-)-ofloxacin within the receiving waters of a wastewater treatment plant (WWTP) indicating potential stereoselective degradation of ofloxacin by bacteria within the WWTP. This possible role of environmental bacteria in enantiomeric enrichment has also been shown through the enantioselective degradation of ofloxacin and levofloxacin by two strains of environmental bacteria (Maia, Tiritan and Castro, 2018). The potential role of stereochemistry in the fate of antibiotics within the environment has been discussed elsewhere (Elder et al., 2020). There is however very little known experimentally about the stereoselectivity of metabolism of antibiotics by bacteria in relation to ABR and its potential impact on the fate of antibiotics within the environment.

In this manuscript chloramphenicol is used as a proof of concept to test the hypothesis that enzymatic antibiotic resistance mechanisms, that have the potential to play a role in the fate of antibiotics within the environment, are stereoselective in nature. Chloramphenicol contains two asymmetric carbons, chloramphenicol can exist as one of four stereoisomers, or a member of two enantiomeric pairs (Figure 1). The *R,R*-(-)-chloramphenicol is the naturally produced stereoisomer and active isomer that is sold within the U.K, whilst all the others have been synthesised (Brock, 1961). Chloramphenicol, its synthesis, mode of action and resistance mechanisms in relation to stereochemistry have been reviewed elsewhere (Elder et al., 2020). This manuscript focusses on

understanding the role stereochemistry plays in the fate of chloramphenicol within the environment through investigating the stereoselectivity of a key bacterial resistance mechanism to chloramphenicol – chloramphenicol acetyltransferase (CAT). CAP is metabolised and deactivated by CAT through the addition of two acetyl groups (Figure 2) which prevent CAP binding to its rRNA 16S target. Both CAP and CAT have been reported in many different environmental compartments (Lu, Dang and Yang, 2009; Szczepanowski et al., 2009; Jiang et al., 2013; Zhou et al., 2013; Le et al., 2018) including within a WWTP catchment in the UK where it was demonstrated that anthropogenic sources of ARGs and ABs are key in driving the presence of ABs and ARGs within aquatic environments (Elder et al., 2021). Here, through utilisation of the stereoselective antimicrobial metabolism (SAM) assay developed by Elder et al (F. C. Elder et al., 2020), we investigated the stereoselective metabolism of chloramphenicol by bacterial strains containing *catA* gene entering WWTPs. This study has increased our understanding of how stereoselective metabolism of antibiotics by anthropogenic bacteria influence the fate of chloramphenicol within a WWTP and its release into the environment.

2. Experimental Section

2.1. Materials

HPLC-grade acetonitrile (>99.9%), HPLC-grade isopropanol (>99.9%), HPLC-grade methanol (>99.9%), HPLC-grade ethanol (>99.9%), ammonium acetate ammonium hydroxide, tryptic soy broth and *RR-p*-chloramphenicol were supplied by Sigma-Aldrich (Gillingham, UK). *SS-p*-chloramphenicol, *R,S-p*-chloramphenicol and *S,R-p*-chloramphenicol was supplied by TRC (Toronto, Canada) and by LGC Standards (Teddington, UK). *D5*(±)-chloramphenicol was supplied by LGC Standards (Teddington, UK). *RR-p*-chloramphenicol acetate was supplied by Santa Cruz Biotechnology (Dallas, USA). Ultrapure water was obtained from a water purification system (MilliQ system UK). Brilliance UTI Chromogenic Agar was supplied in pre-poured plates by Oxoid (Basingstoke, UK). Qiagen QIAmp DNA mini prep kit (Qiagen) was used for DNA extraction and Imumina Nextra XT kit (Illumina) and V3-600 reagent cartridges (Illumina) were used for whole genome sequencing. Stock solutions for each compound were prepared in acetonitrile and stored at -16°C. All glassware used for chemical analysis was deactivated with dimethylchlorosilane (5% DMDCS in toluene, Sigma-Aldrich) (Kasprzyk-Hordern, Dinsdale and Guwy, 2008).

2.2. Methods

2.2.1. Sampling

Influent wastewater samples were collected from two wastewater treatment plants in South West England over three separate weeks in March and July 2018. 24h time proportional autosamplers (ISCO 3700) were used to allow a representative sample collection. Samples were then transported to the laboratory (on ice to maintain low temperature) and immediately processed with biology and chemistry methods as described below.

2.2.2. Isolation of environmental bacteria

BD CLED Agar (Cystine-Lactose-Electrolyte-Deficient Agar) culture medium was used to isolate and enumerate bacteria from wastewater samples. The lack of electrolytes prevents undue swarming bacterial species. 10 µL of wastewater was plated onto CLED agar plates containing 4 mg/L of *RR-p*-chloramphenicol to select for ABR strains. All plates were incubated overnight aerobically at 37°C. Selected colonies were initially identified through overnight growth on Brilliance UTI Chromogenic Agar (aerobically at 37°C) and stored at -80°C on Microbank beads for future analysis.

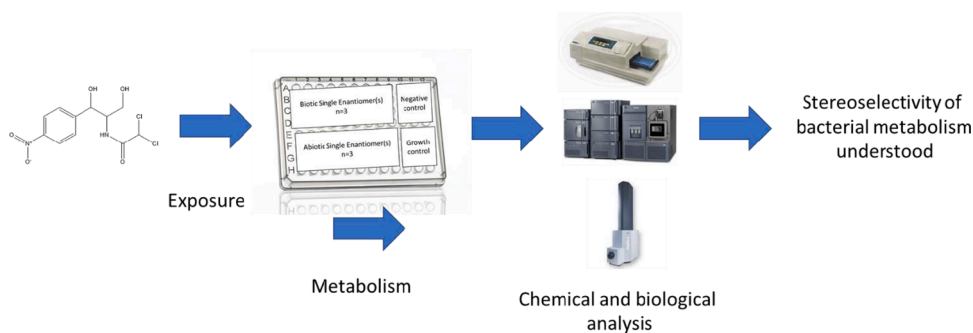


Fig. 3. SAM workflow

2.2.3. Minimum inhibitory concentration (MIC) for 4 chloramphenicol isomers

Bacterial isolates from two WWTPs utilising two different biological treatment processes were grown on CLED agar at 37°C aerobically overnight from Microbank bead. Growth was normalised using a McFarland 0.5 OD (600nm) standard in sterile dH₂O and 50 µL added to 4950 µL TSB to give approximately 1.5×10^6 CFU per mL.

A stock solution of 256 mg/L of each chloramphenicol enantiomer was made in sterile dH₂O. The MIC across a range of 126 - 0.25 mg/L was investigated for each strain via the microbroth method in a 96 well plate. The 96 well plate was incubated aerobically at 37°C for 18 hours and optical density at 600nm read in a Molecular Device SpectraMax3 to indicate growth or no growth. Positive and negative controls were run for each isolate.

2.2.4. DNA extraction and whole genome sequencing

DNA was prepared for whole genome sequencing using Qiagen QIAmp DNA mini prep kit (Qiagen) with lysis step. DNA was then quantified, and quality assessed using the Nanodrop 2000 (ThermoFisher Scientific). Illumina Nextera XT kit, as per manufacturers protocol, was then used to prepare genomic libraries. Sequencing was performed using the Illumina MiSeq platform and V3-600 reagent cartridge to generate 2×250 bp paired-end reads. Reads were assembled using SPades 3.5.0 (Bankevich et al., 2012) and analysed for species and antimicrobial resistance genes present using Edge online platform (Li et al., 2017).

2.2.5. Chemical analysis of chloramphenicol utilising mass spectrometry

Quantification of chloramphenicol isomers RR-p-CAP and S,S-p-CAP with chiral-SFC-QqQ. Analysis of chloramphenicol enantiomers RR-p-CAP and SS-p-CAP was undertaken using Waters UPC² supercritical flow chromatography coupled to Waters Xevo TQD equipped with electrospray ionization source (ESI) mode as described by Elder et al (F. C. Elder et al., 2020). The chromatographic separation of the two enantiomers was achieved using Waters Trefoil Amy1 column (2.5µm, 2.1mm X 50mm) with a mobile phase gradient of CO₂ (A) and 1:1:1 methanol: isopropanol: ethanol with 0.1% ammonium hydroxide (B). The gradient elution used was: 15% B (0-1min), 60% B (1-5min), 60% B (5-7.5 min), 15% B (7.5-7.8 min), 15% B (7.8-9min) with a constant flow rate of 0.7mL/min. Column temperature was set to 30°C and injection volume was 3 µL. The mass spectrometer was operated in MRM (multiple reaction monitoring mode) with an ESI probe set in negative ionisation mode. Optimised ESI parameters for chloramphenicol were as follows: capillary voltage 3.0 kV, source temperature 150°C and desolvation temperature 400°C. Nebulising and desolvation gas was nitrogen. The cone gas flow was 100 L/h and the desolvation gas flow was 550 L/h. Collision gas was argon. MRM transitions for chloramphenicol were 320.8>151.8 (quantitative), 320.8>194.0 (qualitative). MRM transitions for chloramphenicol D5 was 325.9>157.0. The linearity for the analyte concentration range of 5-600 µg/L was $R^2 = 0.995$ (RR) 0.994

(SS) with method detection and quantification limits for chloramphenicol were as follows: MDL = 1 µg/L and MQL = 5 µg/L. Enantiomeric fraction was $0.39 \pm 2.7\%$.

Quantification of chloramphenicol isomers S,R-p-CAP and R,S-p-CAP with chiral-LC-QqQ. Analysis of chloramphenicol enantiomers R,S-p-CAP and S,R-p-CAP was undertaken using Waters Acquity UPLC system coupled to Waters Xevo TQD equipped with electrospray ionization source (ESI) mode. The chromatographic separation of the two enantiomers was achieved using AGP column (100 × 2mm, 5µm) with a mobile phase consisting of 10mM ammonium acetate 90:10 dH₂O and column temperature set at 30°C. An injection volume was 50µL. The mass spectrometer was operated in MRM mode with an ESI set in negative mode. Optimised ESI negative parameters for chloramphenicol were as follows: capillary voltage: 3.0 kV, source temperature: 150°C and desolvation temperature: 400°C. Nebulising and desolvation gas was nitrogen. The cone gas flow was 100 L/h and the desolvation gas flow was 550 L/h. Collision gas was argon. MRM transitions for chloramphenicol were 320.8>151.8 (quantitative), 320.8>194.0 (qualitative). MRM transition for chloramphenicol D5 was 325.9>157.0. The linearity for the analyte concentration range of 5-200 µg/L was $R^2 = 0.853$ (RS), 0.763 (SR) with method detection and quantification limits for chloramphenicol were as follows: MDL = 1 µg/L and MQL = 5 µg/L. Enantiomeric fraction was $0.6 \pm 0.08\%$.

Full chemical profiling and metabolite identification with UPLC-QTOF. Full chemical profiling and metabolite identification of chloramphenicol was performed by UPLC-QTOF using a previously published method (Lopardo et al., 2017). The method utilises a Dionex Ultimate 3000 HPLC (Thermo Fisher, UK, Ltd.) coupled to a Bruker Maxis HD Q-TOF (Bruker) equipped with an electrospray ionization source for all analyses. The nebulising gas was nitrogen with a flow rate of 11 L/min and temperature of 220°C at a pressure of 3 bar. Capillary voltage was 4500V and end plate offset 500V. Analyses were performed in negative mode in both full scan mode (MS) and broadband CID acquisition mode (MS/MS). HyStar Bruker software was used to coordinate the LC-MS system. Chromatographic separation was achieved using Waters ACQUITY UPLC BEH C18 column (50 mm x 2.1 mm, 1.7 µm) with the following mobile phase composition: 1mM ammonium fluoride in water (A) and methanol (B). The flow rate was set at 0.4mL/min and the following gradient was used for the elution of compounds: 5% B (0-3 min), 60% B (3-4 min), 60% B (4-14 min), 98% B (14-17 min), 5% B (17.1-20 min). The source and operating parameters had been optimised as: capillary voltage, 4500 V; dry gas temperature, 220°C (N₂); dry gas flow rate 12 L H⁻¹ (N₂); quadrupole collision energy, 4 eV; collision energy, 7 eV MS (full-scan analysis) and 20 eV MS/MS (bbCID mode). Nitrogen was used as the nebulizing, desolvation and collision gas. The method underwent full validation for the quantification of chloramphenicol and chloramphenicol 3-acetate with chloramphenicol D5 as internal standard where a linearity range of $R^2 = 0.998$ (CAP) and 0.980 (CAP 3-acetate) was achieved within the following analyte

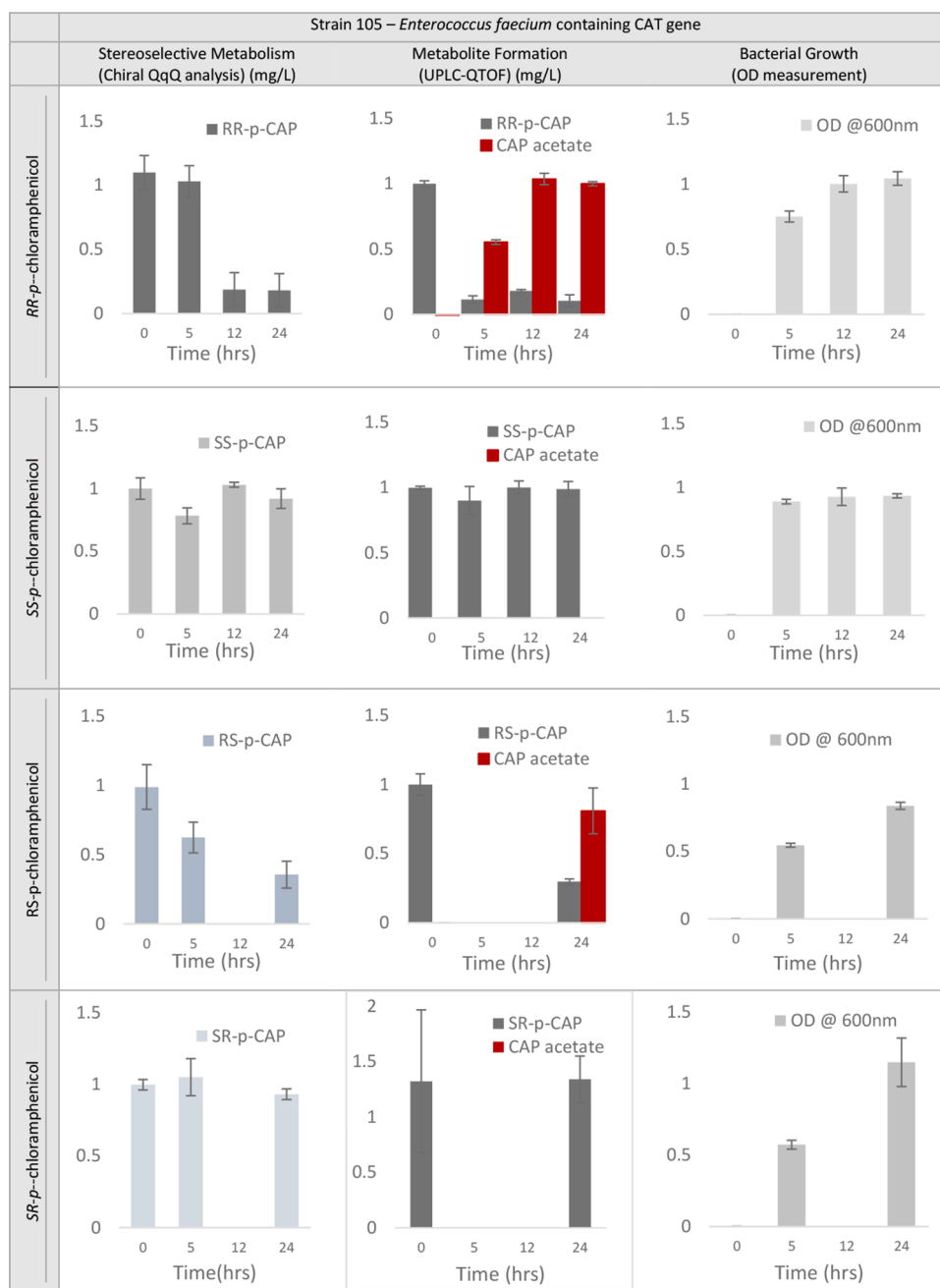


Fig. 4. Investigation of stereoselective metabolism of chloramphenicol by bacterial strain 105 ($n=3$). Results from abiotic controls can be seen in Figure S1 and mass balance in Table S1.

concentration range: 3–100 $\mu\text{g/L}$. Method detection and quantification limits for chloramphenicol were as follows: MDL = 1 $\mu\text{g/L}$ and MQL = 3 $\mu\text{g/L}$. Method detection and quantification limits for chloramphenicol 3-acetate were as follows: MDL = 1 $\mu\text{g/L}$ and MQL = 3 $\mu\text{g/L}$.

2.2.6. Nanocosm

This assay has previously been described by Elder et al (F. C. Elder et al., 2020). Each strain was tested against the four p-CAP isomers: RR, SS, RS and SR. 100 μL of 2 mg/L chloramphenicol (single isomer) and 100 μL of 1.5×10^6 CFU of an individual bacterial strain were added to individual wells of 96 wells of Thermofisher clear bottom microplate to give a final concentration of 1 mg/L chloramphenicol (Figure 3), then incubated in a plate reader at 37°C with shaking. For abiotic controls 100 μL of TSB replaced the addition of bacteria and for growth controls 100 μL of TSB replaced the addition of the antibiotic. Bacteria growth at

37°C was then measured by a Molecular Devices SpectraMax3 plate reader at 600nm every minute over a 24-hour period. The Nanocosms for RR-p-CAP and SS-p-CAP were sampled at four time points (T0h, T5h, T12h and T24h). Samples were diluted 1:10 in methanol with chloramphenicol D4 as an internal standard (100 ng/L), chilled overnight at 5°C and centrifuged for 5 mins at 13000 rpm. The supernatant was aspirated and placed into 500 μL plastic LC vials for analysis by SFC-QqQ. The nanocosm for RS-p-CAP and SR-p-CAP were sampled at 3 time points (T0, T5 and T24). Samples were diluted 1:10 in methanol with chloramphenicol D5 as an internal standard (100 ng/L), chilled overnight at 5°C and centrifuged for 5 mins at 13000 rpm. After aspiration of supernatant, the supernatant was then evaporated under nitrogen and resuspended in mobile phase (10mM ammonium acetate 90:10 dH₂O: ACN) before being analysed within 24hrs by chiral UPLC-QqQ as described by Camacho-Muñoz et al (Camacho-muñoz and

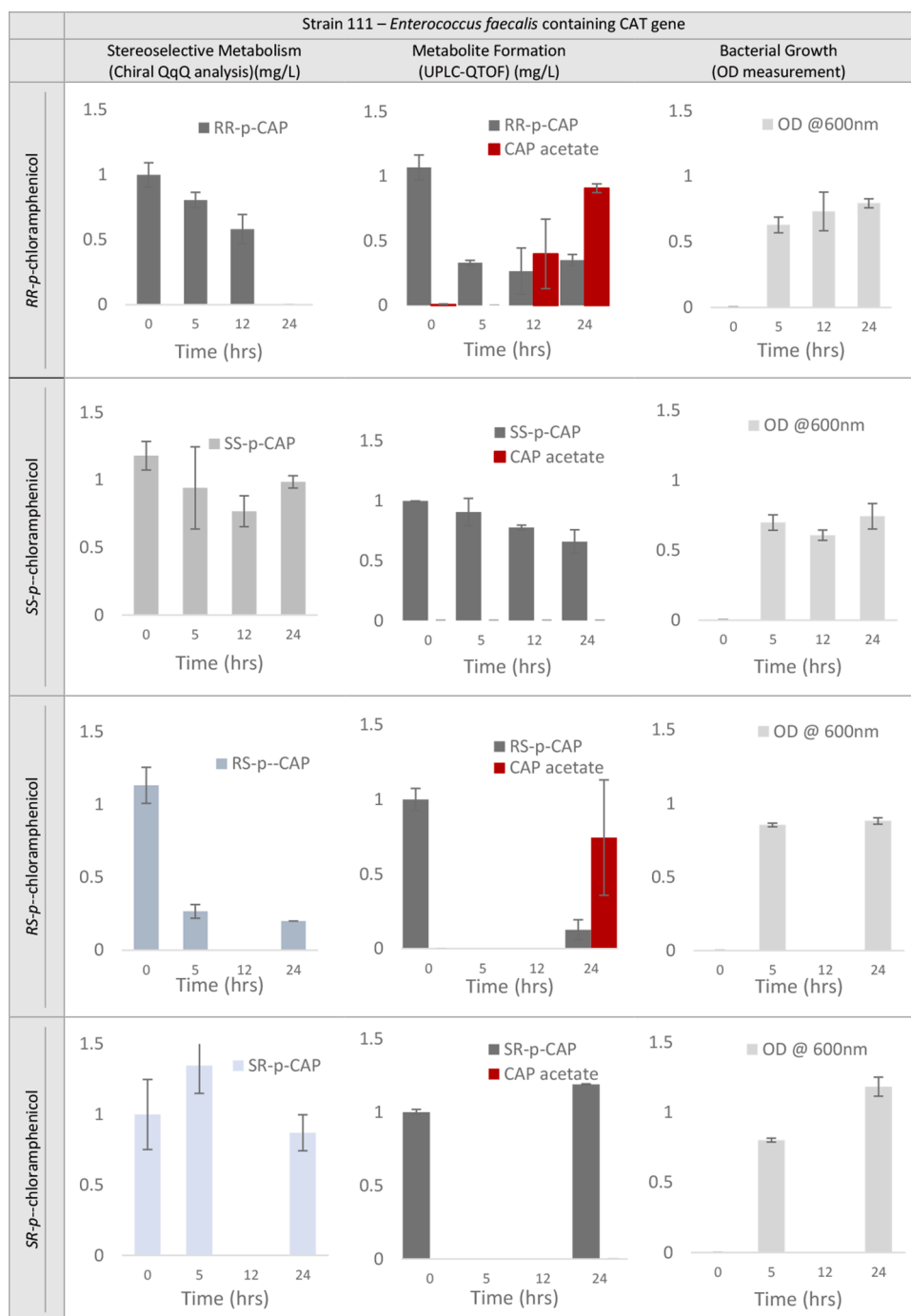


Fig. 5. Investigation of stereoselective metabolism of chloramphenicol by Strain 111(n=3). Results from abiotic controls can be seen in Figure S2 and mass balance in Table S1.

Kasprzyk-hordern, 2015). Statistical analysis was performed for each isomer using Student T-Test: Two-Sample Assuming Equal Variances (two tailed).

2.2.7. Computational analysis of CAP and CAT interactions

To enable visualisation of the binding of different chloramphenicol isomers to chloramphenicol acetate structures were downloaded from RSCB protein data base (PDB) ('10.2210/3CLA/pdb', no date; '10.2210/pbd3u9/pdb', no date). Homotrimers were formed from the symmetry. Heteroatoms other than CAP were eliminated. Hydrogens were added using MolProbity web server at Duke University(Williams et al., 2018). Hydrophobic and polar constraints were identified using the SBFIRST

protocol(McManus, Wells and Walker, 2020) with visualisation with PyMol© Schrodinger LLC. Software ("FLEXOME") for this constraint analysis is available from the University of Bath(Wells, 2022)).

3. Results and Discussion

3.1. Isolation, identification and minimum inhibitory concentrations

Bacteria strains were isolated from influent wastewater from two WWTPs within a river catchment in the South West of England (WWTP A serving 109,543 inhabitants and WWTP B serving 867,244 inhabitants) based on the knowledge that both chloramphenicol and

chloramphenicol acetyltransferase gene have been detected in the influent wastewater from these sites previously (Elder et al., 2021). 19 strains were isolated across the two WWTPs and given an initial identification on Brilliance UTI Chromogenic Agar. The species identified were *Enterococcus* spp (6), *Escherichia coli* (4), *Proteus* spp (4), *Pseudomonas* spp (2) and gram-negative coliforms (3). MICs for the four chloramphenicol enantiomers were then performed for all 19 strains isolated alongside the control strains NCTC 12241 and NCTC 775, see Table 2. Table 2 clearly shows that MICs for individual CAP isomers are isomer and isolated bacteria strain dependent. The lowest MICs were recorded for *RR-p*-CAP, which indicates that this CAP isomer has the highest potency against selected bacteria. Whole genome sequencing was carried out for the 6 strains that had a Brilliance UTI agar identification of *Enterococcus* spp. Three of the strains were identified as *Enterococcus* spp. while the other three were identified as *Serratia* spp. Identification and resistance mechanisms can be found in Table 3. It is interesting to note that the CAT gene encoding chloramphenicol acetyltransferase was only identified in *Enterococcus* spp. a common fecal bacteria but not in with *Serratia* spp.

3.2. Stereoselective transformation of chloramphenicol

The stereoselective metabolism of the *RR-p*- and *SS-p*-CAP enantiomers by the strains 105, 111 and 112 that carry the *catA* gene was investigated in nanocosm experiments using SAM. Strains 100, 101, 244 with no *catA* gene present were used as negative controls. The SAM workflow was subsequently used to investigate the stereoselective metabolism of the other two chloramphenicol isomers *RS-p*-CAP and *SR-p*-CAP, in the strains carrying the *catA* gene (105, 111, 112).

3.2.1. Strain 105 – *catA* carrying

The bacterial strain 105 which was confirmed to contain the *catA* gene was run through the SAM workflow in order to determine if the CAT enzyme present was stereoselective in its transformation of the *RR-p*-CAP and *SS-p*-CAP isomers (Figure 4). The chiral QqQ analysis over a 24-hour period showed a significant reduction of the *RR-p*-CAP isomer with no reduction of the *SS-p*-CAP isomer. Investigation of metabolite formation via UPLC-QTOF analysis after exposure of Strain 105 to the *RR-p*-CAP and *SS-p*-CAP showed formation of the metabolite chloramphenicol acetate when the strain was exposed to the *RR*-enantiomer and not the *S,S*-enantiomer, which clearly shows stereoselective metabolism of *RR-p*-CAP over *SS-p*-CAP, $p = 7.77e-6$. Further investigations were then carried out focussed on the metabolism of the remaining two chloramphenicol isomers, *RS-p*-CAP and *SR-p*-CAP. Here stereoselective metabolism of *RS-p*-CAP was seen alongside formation of the chloramphenicol acetate metabolite. No change in *SR-p*-CAP concentration and no formation of the metabolite was observed indicating that CAT is able to transform only *RR-p*-CAP and *RS-p*-CAP.

3.2.2. Strain 111 – *catA* carrying

Strain 111 was isolated from influent wastewater and full genome sequencing confirmed chloramphenicol resistance was achieved through the presence of a *catA* gene. Using the SAM workflow this strain was exposed to all 4 isomers of chloramphenicol (Figure 5). The analysis for the *R,R-p*- and the *S,S-p*-isomers were performed using chiral-QqQ and showed clear stereoselective metabolism of *R,R-p*-CAP ($P = 3.96e-5$) alongside formation of the metabolite CAP acetate when the strain was exposed to the *R,R-p*-isomer with no formation when exposed to the *S,S-p*-isomer. Further investigations into the metabolism of *R,S* and *S,R-p*-CAP were then carried out using chiral-QqQ. Here stereoselective metabolism of *R,S-p*-CAP was seen alongside formation of the chloramphenicol acetate metabolite when full chemical profiling using UPLC-QTOF was performed.

3.2.3. Strain 112 – *catA* carrying

Through utilising the SAM workflow Strain 112, isolated from

influent wastewater, and confirmed to carry the *catA* gene, was exposed to all four isomers of chloramphenicol (Table 5) The chiral analyses for the *RR-p*-CAP and the *SS-p*-CAP isomers were performed using chiral-QqQ and showed stereoselective metabolism of *RR-p*-CAP but not *SS-p*-CAP ($P = 0.013878$). leading to the formation of the metabolite CAP acetate when the strain was exposed to the *R,R-p*-isomer, with no formation when exposed to the *SS-p*-isomer. Further investigations into the metabolism of *RS-p*-CAP and *SR-p*-CAP were then carried out using chiral-QqQ. Here there appeared to be preference for the metabolism of the *RS-p*-isomer. The investigation of metabolites formed after exposure to the *RS-p*-CAP and the *SR-p*-CAP isomers showed that after 24hrs there was formation of CAP acetate for only the *RS-p*-isomer.

3.2.4. Strain 100, 101, 244 – other chloramphenicol resistance mechanisms than CAT.

Nanocosm experiments were performed for strain 100, 101, 244 for the investigation of the stereoselective metabolism of the *RR-p*-CAP and *SS-p*-CAP isomers. No significant metabolism of either isomer was demonstrated which was to be expected as full genome sequencing did not show the presence of an enzymatic resistance mechanism to CAP.

Due to there being no significant loss of chloramphenicol during chiral analysis, metabolite investigation using UPLC-qTOF was not carried out. Results from abiotic controls can be seen in Figure S4.

3.3. Computational analysis of CAP bound to CAT

To gain a greater understanding around the role stereochemistry plays in the interaction between CAT and CAP computational analysis of CAT bound to different isomers of CAP was performed. Hydrophobic and polar interactions were detected based on interatomic distances, and the polar interaction strength estimated based on the donor-hydrogen-acceptor distances and angles (McManus, Wells and Walker, 2020). The crystal structures of 3U9F (*E. coli* type I CAT complexed with CAP) and of 3CLA (*E. coli* type III CAT complexed with CAP) were chosen for this study as other crystal structures found for CAT variants did not have CAP present. Figures 8 and 9 show the lodging of CAP into the active sites of the two types of CAT. The type I and the type III CAT display the same geometry of CAP in the binding site, with the $-NO_2$ group directed outwards towards the solvent, not forming any interactions with the protein, and the $-C-C12$ group folded back over the aromatic ring. The consistent features of the interaction between CAP and CAT are that (i) the aromatic ring of CAP interacts with hydrophobic residues from “below” i.e. on the side opposite to the chloro- group of CAP; and that (ii) the CAP O4-H forms a hydrogen bond with a neighbouring HIS residue. This visualisation of the binding of CAP to CAT corresponds with the metabolism studies from the SAM assay, *RR-p*-CAP and *RS-p*-CAP metabolised while *SS-p*-CAP and *SR-p*-CAP are not. This suggests that the stereochemistry around the first centre is key for CAP to be complexed into the CAT binding site (Figure 10). If this stereochemistry is wrong, it is not possible to pose CAP within the binding site so as to form the hydrogen bond between O4-H and the HIS acceptor alongside fitting the $-C-C12$ group into an appropriate position.

3.4. Environmental impact

Previous work by the authors had shown *catA* genes to be present in the influent of both WWTPs, while the achiral analysis for CAP showed its presence in the influent wastewater of WWTP B (Elder et al Water Research submitted 2021), Figure 11.

In the same work the authors showed CAP and *catA* to be present in the effluent of both WWTPs (Figure 11). The presence of CAP in the effluent of WWTP A but not in the influent can be explained through cleavage of parent compound from glucuronide metabolite. In WWTPB positive removal of CAP is seen with an average of 54.5% removal over the week, and alongside the presence of *catA* in both influent and effluent wastewater this points towards bacterial metabolism playing a

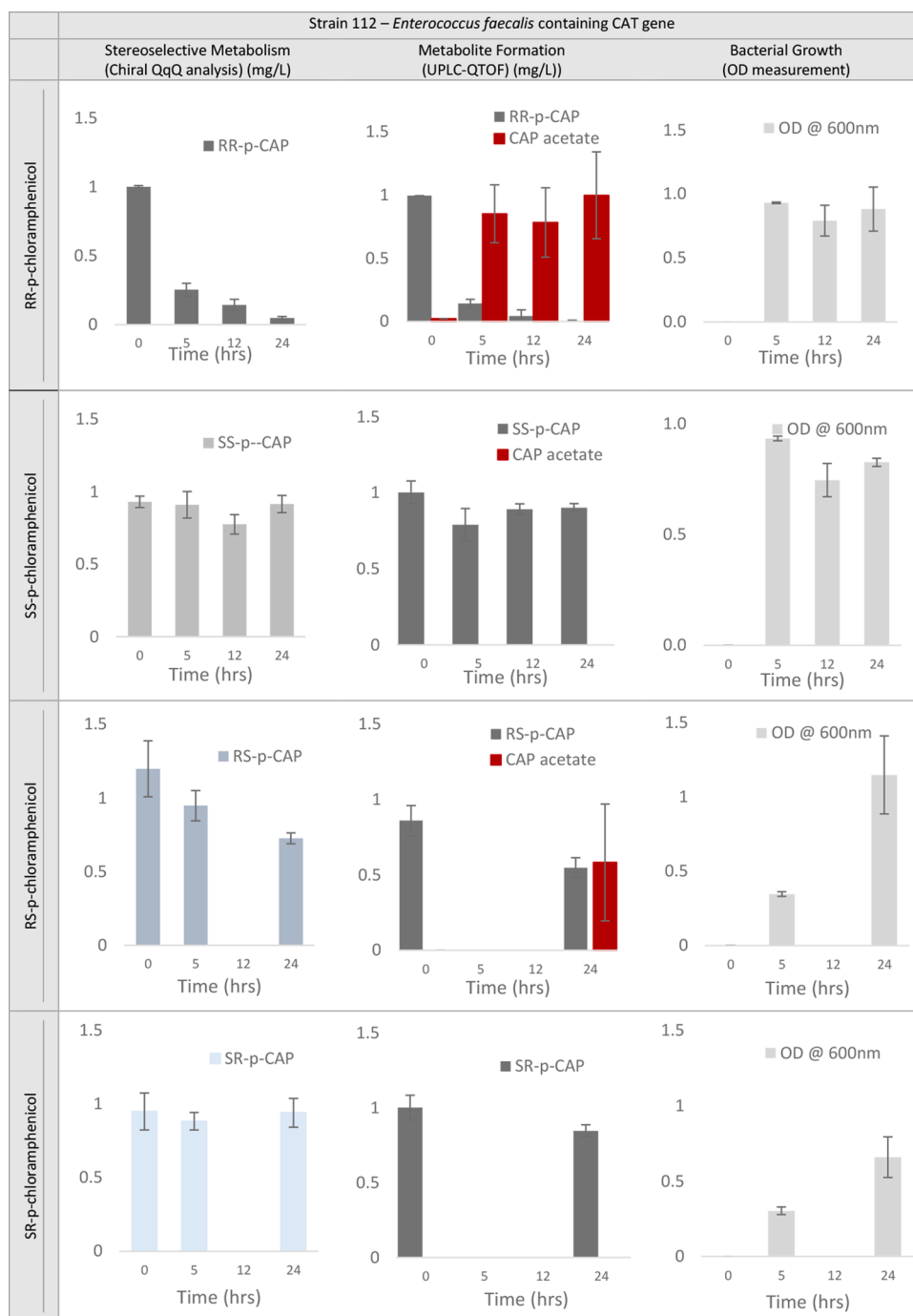


Fig. 6. Investigation of stereoselective metabolism of chloramphenicol by Strain 112 (n=3). Results from abiotic controls can be seen in Figure S3 and mass balance in Table S1.

role in its removal. The presence of CAT and the fact it has been shown to be stereoselective, has potential implications of enantiomeric enrichment within wastewater if multiple CAP isomers are present. This in turn could have implications on ecotoxicity if one isomer is more toxic than another, while the active antibacterial/potent isomer (*RR-p-CAP*) is likely to select for the CAT ARG.

Both WWTPs released CAP and bacterial carrying *catA* genes into the environment. Environmental risk assessments are required for antibiotics under current EMA guidelines (2006) when the predicted environmental concentration exceeds 10 ngL^{-1} . For all chemicals entering the environment the standardised approach for calculating the risk quotient is to divide the measured environmental concentrations (MEC)

by the predicted no effect concentration (PNEC), where the PNEC is determined through a range of standardized tests based on OECD guidelines. OECD guidelines for antibiotics include a range of ecotoxicity tests including on aquatic organisms and an activated sludge respiration inhibition test (ASRIT). While ASRIT assesses the impact ABs may have on the ability of the biological fraction, including bacteria, of a WWTP to treat wastewater, none of the OECD guidelines address the impact ABs have on the development and spread of AMR. This regulatory and knowledge gap in relation to the impact ABs in the environment have on the development and spread of AMR needs to be addressed and it has been proposed that a combination of $\text{PNEC}^{\text{enviro}}$ and PNEC^{MIC} are applied to the ERA for antibiotics (Tell et al., 2019). In this approach the

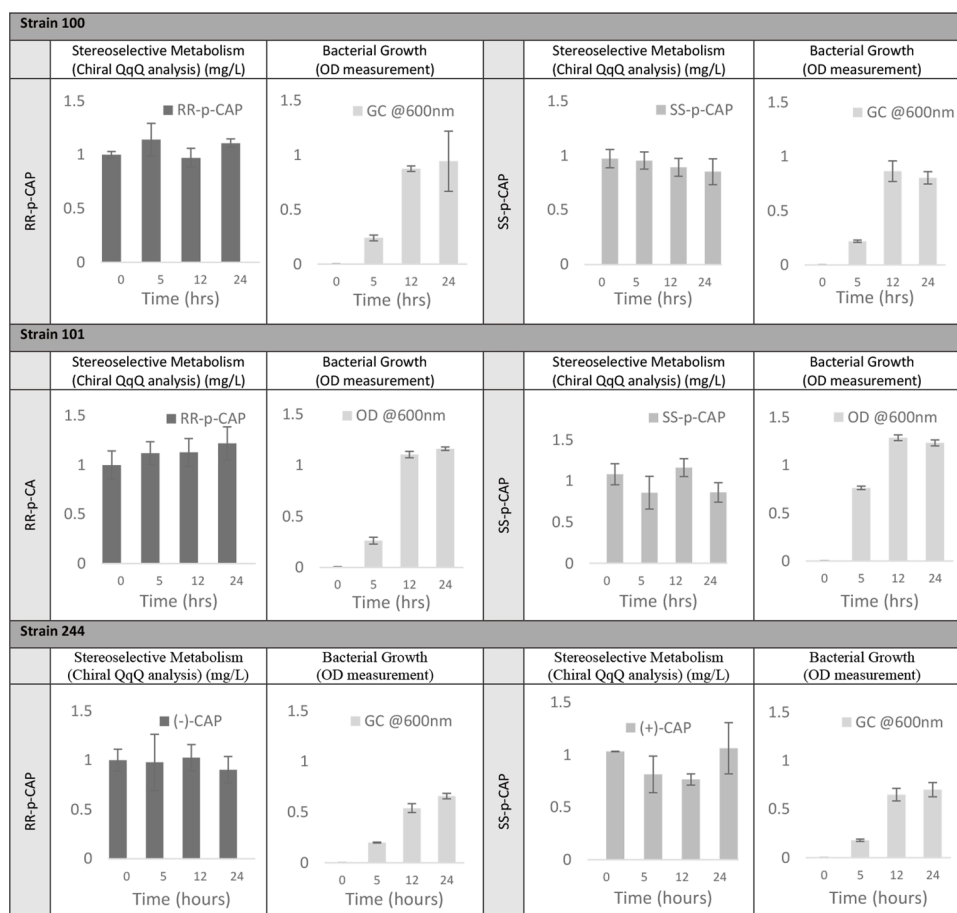
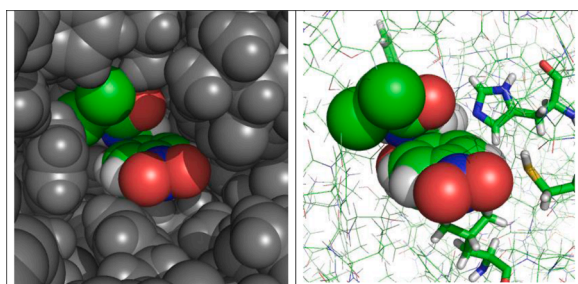
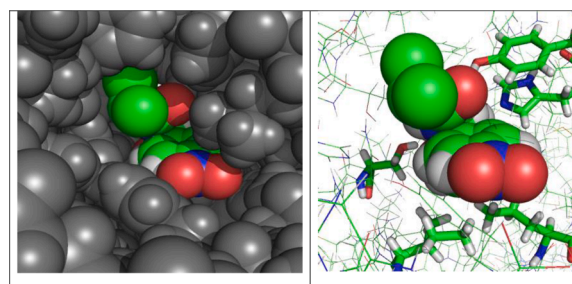


Fig. 7. Investigation of stereoselective metabolism of chloramphenicol by Strains 100, 101 and 244 (n=3).



Left: space-filling view of 3U9F structure, showing CAP lodged in the binding site. The -NO₂ group is directed outward towards solvent. The -C-Cl₂ group is folded back over the aromatic ring.
Right: 3U9F structure shown as lines; residues forming interactions with CAP shown as sticks. CAP (spheres) forms hydrophobic tethers to the side chains of LEU 158 (below) and CYS 31 (right). There is a strong hydrogen bond from CAP O4-H to HIS 193 (upper right), with an estimated strength of -3.13 kcal/mol, and indications of a weak bond from TRP 150 (behind) to CLM O2, with an estimated strength of -0.07 kcal/mol.

Fig. 8. CAP bound in a Type I CAT, 3U9F



Left: space-filling view of 3CLA structure, showing CAP lodged in the binding site. The -NO₂ group is directed outward towards solvent. The -C-Cl₂ group is folded back over the aromatic ring.
Right: 3CLA structure shown as lines; residues forming interactions with CAP shown as sticks. CAP (spheres) forms hydrophobic tethers to the side chains of LEU 160 and ILE 172 (below). There is a hydrogen bond from CAP O4-H to HIS 195 (right), with an estimated strength of -2.33 kcal/mol, and from TYR 25 (upper right) to CAP O2 with an estimated strength of -1.23 kcal/mol. There are indications of a weak bond from SER 148 (behind left) to CLM O5, with an estimated strength of -0.07 kcal/mol.

Fig. 9. CAP bound in a Type III CAT, 3CLA.

PNEC^{enviro} is generated from the standardised ecotoxicology tests whereas the PNEC^{MIC} is derived from EUCAST breakpoint data for antibiotics (Bengtsson-palme and Larsson, 2016) with the lowest of the two PNECs being used to regulate AB levels. Tell et al (Tell et al., 2019) suggested applying the relevant PNEC to the receiving streams. While this approach goes some way to addressing ERAs for ABs that are fit for purpose, where these PNEC^{MICs} are applied within the wastewater system also needs to be addressed as both ARGs and ABs are present in influent wastewater. Stereochemistry of CAP (and other ABs, as most ABs have multiple chiral centres) also requires urgent attention and it

has not been considered so far in the context of ERA for antibiotics. Fig 6-7, Table 1.

4. Conclusions

The main aim of this paper was to undertake a series of assays to characterise the stereoselective metabolism of chloramphenicol by bacterial strains isolated from influent wastewater containing the chloramphenicol acetyltransferase gene.

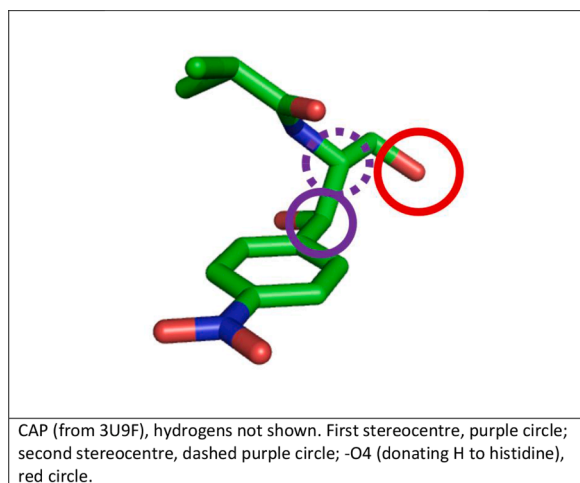


Fig. 10. Key stereochemistry of bound CAP.

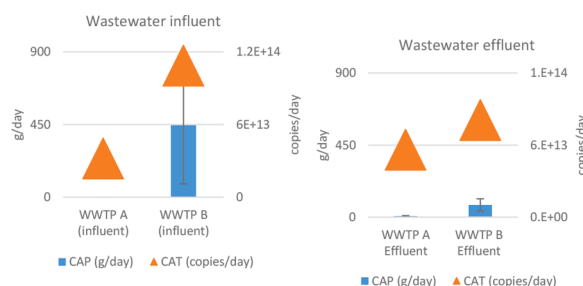


Fig. 11. Daily loads of CAP (g/day, blue) and CAT (copies/day, orange) in wastewater influent and wastewater effluent

- 1 The common chloramphenicol resistance mechanism CAT was shown to stereoselectively transform *RR-p*-CAP and *RS-p*-CAP into the inactive chloramphenicol acetate.
- 2 Metabolism of the *SS-p*-CAP and *SR-p*-CAP isomers by CAT was not shown, indicating the stereochemistry around the first stereocentre is key for the recognition and transformation of CAP by CAT.
- 3 Computational analysis of CAP bound to CAT was performed enabling the visualisation of how the stereochemistry of CAP impacts on the ability of CAT to bind it. This confirmed the metabolism assays findings that the stereochemistry around the first stereocentre is key for recognition of the CAT enzyme.
- 4 Analysis of influent and effluent wastewater for the presence of the *catA* gene and CAP confirmed their presence in wastewater and subsequent release into the receiving environment. Giving the potential for stereoselective transformation to be taking place during wastewater treatment and in the environment further work is needed to fully understand: 1) the enantiomeric fraction of chloramphenicol

within wastewater, 2) if enzymatic recognition of *SS-p*-CAP or *SR-p*-CAP can be induced and 3) the ecotoxicity of different chloramphenicol isomers in order to design an effective ERA for chloramphenicol and other antibiotics.

Funding

Engineering and Physical Sciences Research Council (EP/N509589/1, EP/P028403/1), Natural Environment Research Council (NE/N019261/1), and AstraZeneca Global Safety, Health and Environment are greatly appreciated

CRediT authorship contribution statement

Felicity C T Elder: Conceptualization, Methodology, Formal analysis, Data curation, Writing – original draft, Writing – review & editing. **Ben Pascoe:** Methodology, Writing – review & editing. **Stephen Wells:** Methodology, Formal analysis, Writing – review & editing. **Samuel K Sheppard:** Writing – review & editing. **Jason Snape:** Conceptualization, Supervision, Writing – review & editing. **William H Gaze:** Conceptualization, Supervision, Writing – review & editing. **Edward J Feil:** Conceptualization, Supervision, Writing – review & editing. **Barbara Kasprzyk-Hordern:** Conceptualization, Writing – original draft, Writing – review & editing, Supervision, Project administration, Funding acquisition, Resources.

Table 2

Brilliance UTI Agar Identification and individual isomers of chloramphenicol MICs.

Laboratory Strain Number/WWTP	Identification Brilliance UTI	Minimum Inhibitory Concentration (mg/L)			
		RR-p-CAP	SS-p-CAP	RS-p-CAP	SR-p-CAP
100/WWTP B	<i>Enterococcus</i> spp.	>128	>128	>128	>128
101/WWTP B	<i>Enterococcus</i> spp.	8	128	>128	>128
105/WWTP B	<i>Enterococcus</i> spp.	64	>128	>128	>128
111/WWTP B	<i>Enterococcus</i> spp.	128	>128	128	>128
112/WWTP B	<i>Enterococcus</i> spp.	64	>128	>128	>128
296/WWTP B	<i>E. coli</i>	128	>128	>128	128
301/WWTP B	<i>coliform</i>	>128	>128	>128	>128
304/WWTP B	<i>Proteus</i> spp.	128	>128	>128	>128
305/WWTP B	<i>E. coli</i>	128	>128	>128	>128
311/WWTP B	<i>E. coli</i>	16	>128	>128	>128
315/WWTP B	<i>Proteus</i> spp.	64	>128	>128	>128
318/WWTP B	<i>E. coli</i>	>128	>128	>128	>128
320/WWTP B	<i>Proteus</i> spp.	>128	>128	>128	>128
324/WWTP B	<i>coliform</i>	128	>128	>128	>128
325/WWTP B	<i>Pseudomonas</i> spp.	32	>128	>128	>128
241/WWTP A	<i>coliform</i>	32	>128	>128	>128
254/WWTP A	<i>coliform</i>	32	>128	>128	>128
244/WWTP A	<i>Enterococcus</i> spp.	64	>128	>128	>128
245/WWTP A	<i>Pseudomonas</i> spp.	8	128	>128	>128

Table 1

Method performance: Chiral SFC- QqQ, Chiral-LC-QqQ, UPLC-QTOF

Methods	CAP	Linearity range[mg/L]	R2	MDL[mg/L]	MQL[mg/L]	Accuracy [%](intraday)	Precision [%](intraday)
Chiral SFC- QqQ	RR-p-CAP	5-600	0.995	0.001	0.005	2.8	7.1
	SS-p-CAP	5-600	0.995	0.001	0.005	11.7	2.3
Chiral-LC-QqQ	SR-p-CAP	5-200	0.763	0.001	0.005	10.0	15.0
	RS-p-CAP	5-200	0.853	0.001	0.005	10.0	15.0
UPLC-QTOF	RR-p-CAP	3-100	0.998	0.001	0.003	10.0	5.0
	SS-p-CAP	3-100	0.998	0.001	0.003	10.0	5.0
	SR-p-CAP	3-100	0.998	0.001	0.003	10.0	5.0
	RS-p-CAP	3-100	0.998	0.001	0.003	10.0	5.0

Table 3
Identified antibiotic resistance mechanisms of *Enterococcus* spp. and *Serratia* spp isolated from wastewater.

Strain	Full Identification	Antibiotic resistance mechanisms
Strain 100	<i>Serratia liquefaciens</i> (Identification Brilliance UTI agar as <i>Enterococcus</i> spp.)	Class C Beta-Lactamase, MFS Antibiotic Efflux
Strain 101	<i>Serratia liquefaciens</i> (Identification Brilliance UTI agar as <i>Enterococcus</i> spp.)	ABC Antibiotic Efflux, MFS Antibiotic Efflux, Quinolone Resistance, Class C Beta-Lactamase, Tetracycline Ribosomal Protection
Strain 105	<i>Enterococcus faecium</i>	CAT Group A, Aminoglycoside Phosphotransferase, rRNA Methyltransferase, Tetracycline Ribosomal Protection, MFS Antibiotic Efflux, Aminoglycoside Nucleotidyltransferase, ABC Antibiotic Efflux
Strain 111	<i>Enterococcus faecalis</i>	CAT Group A, ABC Antibiotic Efflux, MFS Antibiotic Efflux, Tetracycline Ribosomal Protection, Aminoglycoside Nucleotidyltransferase, rRNA Methyltransferase, Aminoglycoside Acetyltransferase, Aminoglycoside Phosphotransferase
Strain 112	<i>Enterococcus faecalis</i>	CAT group A, MFS Antibiotic Efflux, Lincosamide Resistance, ABC Antibiotic Efflux, Tetracycline Ribosomal Protection, Aminoglycoside Nucleotidyltransferase, rRNA Methyltransferase, Tetracycline Efflux, Aminoglycoside Acetyltransferase
Strain 244	<i>Serratia liquefaciens</i> (Identification Brilliance UTI agar as <i>Enterococcus</i> spp.)	MFS Antibiotic Efflux, Aminoglycoside Phosphotransferase

Declaration of Competing Interest

The authors declare that they have no known competing financial interests or personal relationships that could have appeared to influence the work reported in this paper.

Acknowledgements

Support from Engineering and Physical Sciences Research Council (EP/N509589/1, EP/P028403/1), Natural Environment Research Council (NE/N019261/1), and AstraZeneca Global Safety, Health and Environment is greatly appreciated. The authors would like to thank Waters for support and provision of ACQUITY UPC² System for the study. MC² for support and provision of UPLC-QTOF for this study.

Supplementary materials

Supplementary material associated with this article can be found, in the online version, at doi:10.1016/j.watres.2022.118415.

References

Andrés-Costa, M.J., et al., 2017. Enantioselective transformation of fluoxetine in water and its ecotoxicological relevance. *Sci. Rep.* 7 (1), 1–13. <https://doi.org/10.1038/s41598-017-15585-1>.
Bagnall, J., et al., 2013. Stereoselective biodegradation of amphetamine and methamphetamine in river microcosms. *Water Res.* 47 (15), 5708–5718. <https://doi.org/10.1016/j.watres.2013.06.057>.

Bankevich, A., et al., 2012. SPAdes: A new genome assembly algorithm and its applications to single-cell sequencing. *J. Comput. Biol.* 19 (5), 455–477. <https://doi.org/10.1089/cmb.2012.0021>.
Bengtsson-palme, J., Larsson, D.G.J., 2016. Concentrations of antibiotics predicted to select for resistant bacteria : Proposed limits for environmental regulation. *Environ. Int.* 86, 140–149. <https://doi.org/10.1016/j.envint.2015.10.015>.
Brock, T.D., 1961. Chloramphenicol. *Bacteriol. Rev.* 25 (1), 32–48.
Camacho-muñoz, D. and Kasprzyk-hordern, B. (2015) 'Multi-residue enantiomeric analysis of human and veterinary pharmaceuticals and their metabolites in environmental samples by chiral liquid chromatography coupled with tandem mass spectrometry detection', pp. 9085–9104. doi: 10.1007/s00216-015-9075-6.
Castrignanò, E., et al., 2018. Enantioselective fractionation of fluoroquinolones in the aqueous environment using chiral liquid chromatography coupled with tandem mass spectrometry. *Chemosphere* 206 (0), 376–386. <https://doi.org/10.1016/j.chemosphere.2018.05.005>.
Elder, F. C. et al. (2020) 'A novel biochemical assay for investigation of stereoselective bacterial metabolism of antibiotics'.
Elder, F.C.T., et al., 2020. The role of stereochemistry of antibiotic agents in the development of antibiotic resistance in the environment. *Environ. Int.* 139 (March), 105681 <https://doi.org/10.1016/j.envint.2020.105681>.
Elder, F.C.T., et al., 2021. Spatiotemporal profiling of antibiotics and resistance genes in a river catchment: human population as the main driver of antibiotic and antibiotic resistance gene presence in the environment. *Water Res.*, 117533 <https://doi.org/10.1016/j.watres.2021.117533>.
Evans, S.E., Bagnall, J., Kasprzyk-Hordern, B., 2016. Enantioselective degradation of amphetamine-like environmental micropollutants (amphetamine, methamphetamine, MDMA and MDA) in urban water. *Environ. Pollut.* 215, 154–163. <https://doi.org/10.1016/j.envpol.2016.04.103>.
Fessner, W.D., et al., 2015. Enzymatic deamination of d-coronamic acid: Stereoselectivity of 1 -aminocyclopropane-1 -carboxylate deaminase. *Perspectives in Sci.* 35 (3), 194–204. <https://doi.org/10.3109/03602532.2014.984814>.
González-Zorn, B., Escudero, J.A., 2012. Ecology of antimicrobial resistance: humans, animals, food and environment. *Int. Microbiol.* 15 (3), 101–109. <https://doi.org/10.2436/20.1501.01.163>.
Helmchen, G., 2016. The 50th anniversary of the cahn-ingold-prelog specification of molecular chirality. *Angewandte Chemie - Int. Edition* 55 (24), 6798–6799. <https://doi.org/10.1002/anie.201603313>.
Honma, M., et al., 1979. Enzymatic deamination of d-coronamic acid: Stereoselectivity of 1 -aminocyclopropane-1 -carboxylate deaminase. *Agric. Biol. Chem.* 43 (8), 1677–1679. <https://doi.org/10.1080/00021369.1979.10863687>.
Jiang, L., et al., 2013. Prevalence of antibiotic resistance genes and their relationship with antibiotics in the Huangpu River and the drinking water sources, Shanghai, China. *Sci. Total Environ.* 458–460, 267–272. <https://doi.org/10.1016/j.scitotenv.2013.04.038>.
Kasprzyk-Hordern, B., Dinsdale, R.M., Guwy, A.J., 2008. Multiresidue methods for the analysis of pharmaceuticals, personal care products and illicit drugs in surface water and wastewater by solid-phase extraction and ultra performance liquid chromatography-electrospray tandem mass spectrometry. *Anal. Bioanal. Chem.* 391 (4), 1293–1308. <https://doi.org/10.1016/j.talanta.2007.08.037>.
Koeller, K.M., Wong, C.H., 2001. Enzymes for chemical synthesis. *Nature* 409 (6817), 232–240. <https://doi.org/10.1038/35051706>.
Le, T.H., et al., 2018. Removal of antibiotic residues, antibiotic resistant bacteria and antibiotic resistance genes in municipal wastewater by membrane bioreactor systems. *Water Res.* 145, 498–508. <https://doi.org/10.1016/j.watres.2018.08.060>.
Li, P.E., et al., 2017. Enabling the democratization of the genomics revolution with a fully integrated web-based bioinformatics platform. *Nucleic Acids Res.* 45 (1), 67–80. <https://doi.org/10.1093/nar/gkw1027>.
Lopardo, L., et al., 2017. New analytical framework for verification of biomarkers of exposure to chemicals combining human biomonitoring and water fingerprinting. *Anal. Chem.* 89 (13), 7232–7239. <https://doi.org/10.1021/acs.analchem.7b01527>.
Lu, X.W., Dang, Z., Yang, C., 2009. Preliminary investigation of chloramphenicol in fish, water and sediment from freshwater aquaculture pond. *Int. J. Environ. Sci. Technol.* 6 (4), 597–604. <https://doi.org/10.1007/BF03326100>.
Maia, A.S., Tiritan, M.E., Castro, P.M.L., 2018. Enantioselective degradation of ofloxacin and levofloxacin by the bacterial strains *Labrys portucalensis* F11 and *Rhodococcus* sp. FP1. *Ecotoxicol. Environ. Saf.* 155 (February), 144–151. <https://doi.org/10.1016/j.ecoenv.2018.02.067>.
Manaia, C.M., et al., 2018. Antibiotic resistance in wastewater treatment plants: tackling the black box. *Environ. Int.* 115 (April), 312–324. <https://doi.org/10.1016/j.envint.2018.03.044>.
McManus, T.J., Wells, S.A., Walker, A.B., 2020. Salt bridge impact on global rigidity and thermostability in thermophilic citrate synthase. *Phys. Biol.* 17 (1) <https://doi.org/10.1088/1478-3975/ab2b5c>.
Qiao, M., et al., 2018. Review of antibiotic resistance in China and its environment. *Environ. Int.* 110 (October 2017), 160–172. <https://doi.org/10.1016/j.envint.2017.10.016>.
Ribeiro, A.R., et al., 2013. Enantioselective biodegradation of pharmaceuticals, alprenolol and propranolol, by an activated sludge inoculum. *Ecotoxicol. Environ. Saf.* 87, 108–114. <https://doi.org/10.1016/j.ecoenv.2012.10.009>.
Rice, J., et al., 2018. Stereochemistry of ephedrine and its environmental significance: Exposure and effects directed approach. *J. Hazard. Mater.* 348 (September 2017), 39–46. <https://doi.org/10.1016/j.jhazmat.2018.01.020>.
Szczepanowski, R., et al., 2009. Detection of 140 clinically relevant antibiotic-resistance genes in the plasmid metagenome of wastewater treatment plant bacteria showing reduced susceptibility to selected antibiotics. *Microbiology* 155 (7), 2306–2319. <https://doi.org/10.1099/mic.0.028233-0>.

- Tell, J., et al., 2019. Science-based targets for antibiotics in receiving waters from pharmaceutical manufacturing operations. *Integrated Environ. Assess. Manage.* 15 (3), 312–319. <https://doi.org/10.1002/ieam.4141>.
- Wells, S., 2022. FLEXOME software suite first release 23/11/2020 Bath: University of Bath. <https://doi.org/10.15125/BATH-00940>.
- Williams, C.J., et al., 2018. MolProbity: More and better reference data for improved all-atom structure validation. *Protein Sci.* 27 (1), 293–315. <https://doi.org/10.1002/pro.3330>.
- Zhou, L.-J., et al., 2013. Occurrence and fate of eleven classes of antibiotics in two typical wastewater treatment plants in South China. *Sci. Total Environ.* 452–453, 365–376. <https://doi.org/10.1016/j.scitotenv.2013.03.010>.